MULTI-SCALE MODEL OF CRACK PROPAGATION IN UNIDIRECTIONAL METALLIC MATRIX COMPOSITES

J.F. Maire, P. Levasseur, P. Paulmier

Office National d'Etudes et de Recherches Aérospatiales
Structures and Damage Mechanics Department
29, Avenue de la Division Leclerc – BP 72
92322 Châtillon - France

ABSTRACT

Fatigue tests have been performed on SiC/Ti composite. They provide an accurate measure of the crack length and a reliable answer of the crack growth. A characteristic crack propagation has been obtained due to the presence of a fibre bridging. A two-scale model has been developed to take bridging influence into account. It is based on linear fracture Mechanics combined to the determination of the closure pressure exerted by the fibres. At the lower scale, pertinent interfacial properties have been described such as debonding and friction. The abilities of this model are in agreement with the different experimental stages. It offers promising prospects to find optimal interfacial properties and to establish a propagation law for bridged cracks.

INTRODUCTION

Under low longitudinal loads, fatigue cracks propagate through CMM's composites, perpendicularly to the fibres. The initiation comes from initial flaws: for instance brittle reaction product at the interface, or an early fibre rupture [1-2]. This damage does not involve a catastrophic failure even if its size is the same as the structural material. Most fibres bridge the matrix cracks, which can allow a stable crack growth. In order to answer at the issue of the tolerance damage for aerospace applications, a first point to overcome is the determination of the crack propagation law for these composites. The bridging fibres exert a closure pressure on the crack surfaces that may reduce substantially the matrix crack growth. In this case, the usual representation of the crack growth versus the amplitude of the Stress Intensity Factor (SIF) differs from the standard Paris' law. Three trends have been observed from experimental results [3]:

- a growth decreasing which can lead to the arrest of the crack
- a steady-state characterised by a constant growth
- a growth increasing which is interpreted as the consequence of bridging fibre ruptures.

The enhancement of fracture toughness by bridging fibres depends strongly on interfacial properties. Weak interfaces with the development of short debonding lengths in the wake of the crack, appear to be the most promising. An efficient fibre bridging is obtained thanks to the dissipation by friction at interfaces and the delay of fibre ruptures [4,5].

In this paper, fatigue tests have been conducted on titanium matrix composite which the interface fibre/matrix exhibits weak mechanical properties. A characteristic bridging behaviour has been observed and analysed. In a second part, a bridged crack model is proposed from a modified Paris' law. The mechanical efforts of the bridging fibres are explicitly take into account for the calculation of the SIF at the crack tip. An important relation to solve the problem is to express the relation between the pressure sustained by the bridging fibres and the crack opening displacement (COD): $\boldsymbol{P(\delta)}$**.** This relation is described using a micromechanical model which differs from previous analysis [6,7]. Attention has been paid to take interfacial behaviour and residual stresses into account orientation after manufacturing process and they are regularly spaced in the matrix. This multiscale approach is described on figure 1.

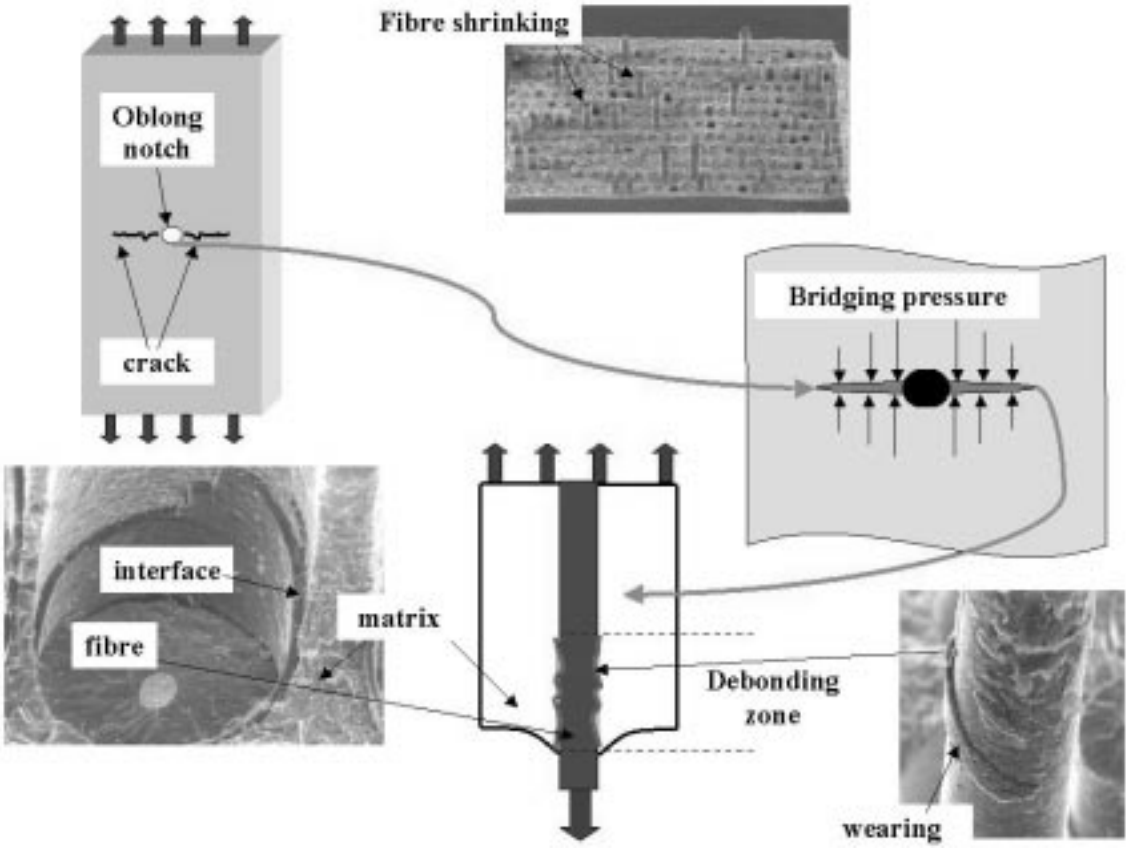

Figure 1: The various scales related to study the bridged crack propagation.

EXPERIMENTAL PROCEDURE

A titanium alloy reinforced with SiC fibre has been tested by fatigue. The unidirectional composite has been elaborated at SNECMA using hot pressing. The fibres keep the same orientation after manufacturing process and are regularly spaced in the matrix. The composite exhibits a transversal isotropic behaviour around the fibre axis. The interface fibre/matrix rich in carbon maintains weak resistance and is subjected to debonding under a low stress state. Furthermore, the interface is initially in radial compression due to the residual stresses. During processing, the thermal expansion mismatch between the fibre and the matrix produces important residual thermal stresses. Consequently, after complete debonding, interfacial friction should occur during the fibre/matrix sliding. On the other hand, in the axial direction, the fibre is in compression where as the matrix is in tension. This residual stress state tends to open a matrix crack perpendicular to the fibres.

The composite is cut along to fibre axis to obtain a parallelepipedic specimen with a total length of 160 mm and a cross section of 8 mm x 2.1 mm. The polishing to one micron surface finish allows an optical observation of the cracked face. An elliptic centre notch is realised through the all specimen thickness by microwaves in order to initiate the fatigue crack. The specimen is loaded parallel to the fibre direction, the traction cycles being controlled by stress levels. The test sample is developing a crack across its width through its all thickness (see figure 2).

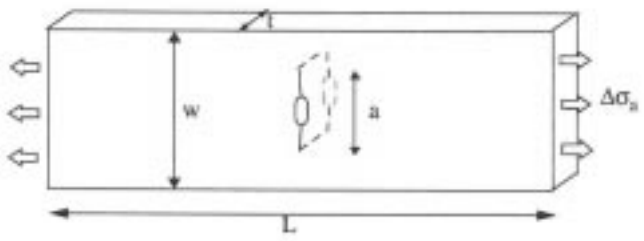

Figure 2: Representation of the experimental specimen

A self-activating optical process measures the crack length. Several images are taken across the cracked width by a CDD camera. The displacements of the camera and the triggers of snapshots are monitoring by a computer. After unitising all images, a cracked width panorama with a resolution of 1000 pixels for one inch is obtained (see figure 3). Afterwards, the use of standard image processing operations allows to locate the crack tips and to carry out an accurate measure of the crack length.
The crack growth rate is calculated by a method according to the ASTM norm. It consists in an interpolation over n centred points. The optimal number of points corresponds to a compromise between an erratic trend for the local measure and a smooth one for average measure, usually n=5 gives a reliable answer. The experimental crack growth curves have been obtained for tests performed at 400°C and at room temperature under a frequency of 50 Hz. At theses temperature no chemical reaction such as oxidation occurs.
The matrix crack exhibits a stable growth and spans over the whole width of specimen without causing its failure. These features are representative to a full-bridged crack where almost all the bridging fibres remain intact. The acceleration stage described by Ghonem [8] has not been attained, in the case the furthest fibre from the crack tip would be broken in the wake of the crack, which could lead to a catastrophic failure.

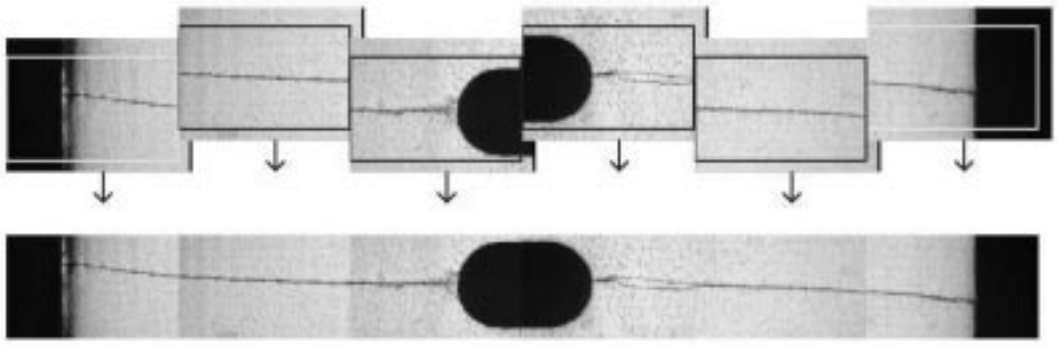

Figure 3: cracked width panorama from image recording.

Furthermore, another notable feature is the fracture surface after complete breaking the specimen. In examining the interfacial region, the debonding happened at different locations: between the carbon layer and the fibre or between the carbon layer and the matrix (see micrographs on figure 1). The presence of fibre roughness indicates that wear effects probably occurred during the test. On the other hand, the fibre pull-out lengths are randomly spaced without pronounced area. This confirms that a stable cracking happened and the acceleration phases are not a result of fibre rupture events. Three parts depicted the crack growth curve:

- In the first one, a neat deceleration occurs; the first points are excluded due to the experimental errors at the test beginning. The bridging has a significant shielding effect over the driving force and its influence is increasing when the crack is growing. At room temperature the crack has even been stopped. For this material, the bridging has a leading role on the crack propagation. In addition, the temperature is a significant parameter: the crack growth is higher at higher temperature. Other works [8,9] has already reported this observation.
- In the second one, a steady state is reached maintaining a constant crack growth. A balance has been established between the acceleration effect due to the growing of the crack and the deceleration effect due to the bridging fibres.
- In the third one, although no fibre breaks, a slight acceleration happens when the crack reaches the edge of the specimen. This suggests that for high ΔKa the bridging effect is less efficient.

On the other hand, at a smaller size scale, acceleration sequences and deceleration sequences follow in turn. The period of this fluctuation is about the width of the elementary cell. This indicates that the growth rate is modified when the crack is bypassing a row of fibres. Several causes may be responsible for this phenomenon: the deflection of the crack, the local fibre volume fraction, the variation of matrix residual stresses or the blunting of the crack tip.

MECHANICAL MODEL

General description

This model is written in the frame of the Linear Elastic Fracture Mechanics. The composite is treated as a homogenous elastic medium where a matrix crack is propagating in mode I. Matrix plasticity is not considered and the plastic zone at the crack tip is supposed to remain small.
A modified Paris' law governs the crack growth:

$$\frac{\partial a}{\partial n} = c\left\langle \Delta K_{tip} - K_s \right\rangle^n \tag{1}$$

where ΔK_{tip} is the effective amplitude at the crack tip caused by combination of the external loading and the axial bridging stresses. The constants *c*, n and the threshold K_s depend only on matrix properties.
To model the mechanical contribution of the bridging fibres on ΔK_{tip}, two scales are used (figure 4): the first one is the crack scale, at the level of the specimen and the second one is the micro scale, at the level of the constituents (fibre, matrix and interface).

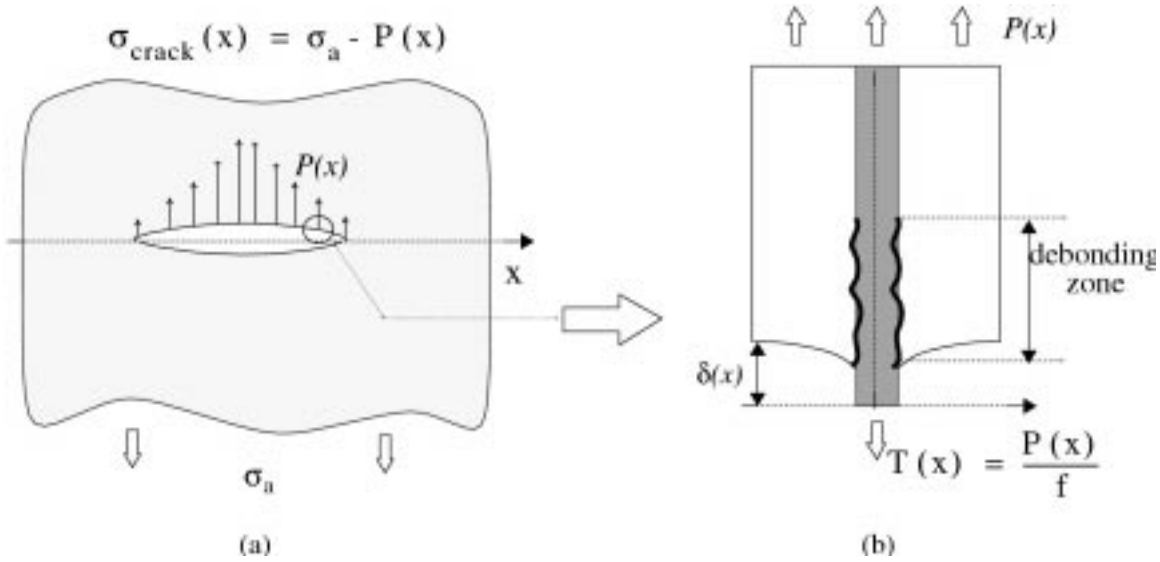

Figure 4: Representation of the two scales: (a) crack scale, (b) micro scale

Crack scale

The discrete fibre stresses applying on the crack surfaces are replaced by a continuous distribution of pressure ***P(x).*** This approximation is valid as long as the fibres exhibit a periodic location and their spacing distance is small compared to the crack length. By the principle of linear superposition, the neat force on the crack surfaces is $\sigma_{crack}(x) = \sigma_a - P(x)$ where σ_a is the external stress and x locates the position on the crack (see Fig 4a). ***P*** is counted negative when it tends to close the crack and positive for the opposite case. The Stress Intensity Factor can be expressed by $K = \int_0^a h(x,a,w) \cdot \sigma_{crack}(x) dx$ where h(x,a,w) is the weight function [11]. Therefore, ΔK_{tip} takes the following expression:

$$\Delta K_{tip} = \Delta K_a - \Delta K_b \tag{2}$$

with $\Delta K_a = \Delta\sigma_a \cdot F(a,w)$ and $\Delta K_b = \int_0^a h(x,a,w).\Delta P(x) dx$

Furthermore, the crack opening displacement (COD) can be expressed according to Rice's relation [10]:

$$\delta(x) = 1/E^* \int_x^a h(x,s,w).\left\{ \int_0^s h(t,s,w)(\sigma_a - P(x))dt \right\} ds \tag{3}$$

where E* is homogenous at a Young modulus. It depends on the anisotropy of the material.

Micro scale

At the micro scale, an elementary cell is used to describe the behaviour of a bridging element surrounded by matrix. It provides a relation between the continuous pressure ***P(x)***, introduced at the crack level, and the crack opening displacement ***δ(x)***. The force balance over a cell section requires that an axial stress of $T(x) = \frac{P(x)}{f}$ is exerting on the bridging fibre at the crack plan (figure 4b.). The COD results from the fibre/matrix sliding at the interface. Two relevant features: the residual stresses and the interfacial behaviour, are taken into account to obtain the response $P(\delta)$ of the bridging element.

The residual stresses are expected to be only generated by the thermal mismatch between the fibre and the matrix during the manufacturing process. They are evaluated thanks to an elastic calculation under generalised plane strains. The interface is supposed to be in compression after this process that means we only consider composites for which the matrix expansion coefficient is greater than the fibre one.

The interfacial behaviour is described by considering the propagation of a debonding zone which friction occurs in. Debonding is expressed under pure shear mode with an ONERA's model. It has been developed from Tvergaard's analysis [11] and further details are available in Ref. [12,13]. A damage variable, λ, is introduced to describe continuously the interfacial debonding from a sound state (λ=0) to a broken one (λ=1). It is controlled by jump displacements at the interface. In the present case, it depends only on the tangential displacement or sliding displacement $\boldsymbol{U_t}$: $\lambda = 1 - \left\langle 1 - \frac{U_t}{\delta_t} \right\rangle$ where δ_t is the sliding displacement, which leads to rupture. During the evolution of λ, the shear resistance of the bond reaches a maximal level $\boldsymbol{\tau_{max}}$ before to go down to the friction level.

After complete debonding, friction is taking place as long as the two surfaces stay in contact. This model uses the Coulomb's law: $\tau_i = \pm\mu\langle -\sigma_r \rangle$. The normal stress, σ_r, depends on the residual radial stress and the Poisson's contraction effect which is not usually negligible [14]. Analytical solution of ***P(δ)*** are obtained from the micromechanical analysis developed by [15]. It is based on the determination of the axial fibre stress σ_f and its integral along the debonding zone, which is proportional to the COD. A key relation is the load transfer of σ_f due to interfacial shear stress:

$$\frac{d\sigma_f}{dz} = \pm \frac{2\tau_i}{r_f} \qquad (4)$$

where **z** is the interface abscise and $\boldsymbol{r_f}$ the fibre radius. The determination of $\boldsymbol{\tau_i}$ leads to solve the whole problem. It depends on interfacial behaviour and history through the loading sequences: monotonic loading or unloading/reloading sequences. During the loading, the debonding length, $\boldsymbol{l_d}$, is extending and $\boldsymbol{\tau_i}$ is given by the debonding model coupled with friction. During cyclic sequences, a reverse slip, $\boldsymbol{l_r}$, is growing from the crack plan where the direction of sliding becomes opposite. This implies a sign change of $\boldsymbol{\tau_i}$ [16]. A notable feature of this analytical solution is that the stress field at the debonding tip is completely described and no jumping stress is introduced, as it is usually proposed in micromechanical models [16].

The initial opening when *P=0* is due to the presence of residual stresses which tend to open the crack because the matrix is initially in tension. For the loading sequence, both G_{II} and μ influence the shape of the curve of ***P(δ)***. For a cyclic sequence, friction causes a hysteresis loop characteristic of energy dissipation. It affects the response as long as the reverse slip, $\boldsymbol{l_r}$, is lower than the debonding length, $\boldsymbol{l_d}$. When $\boldsymbol{l_r}$ reaches $\boldsymbol{l_d}$ an elastic behaviour takes place. In the remaining sections, the relation ***P(δ)*** will be designed by:

$$\delta(x) = \Re_{micro}(P(x)) \qquad (5)$$

where the function $\Re_{micro}$ depends on interface parameters $\boldsymbol{(G_{II}, \mu, \delta_t)}$ and constituent properties.

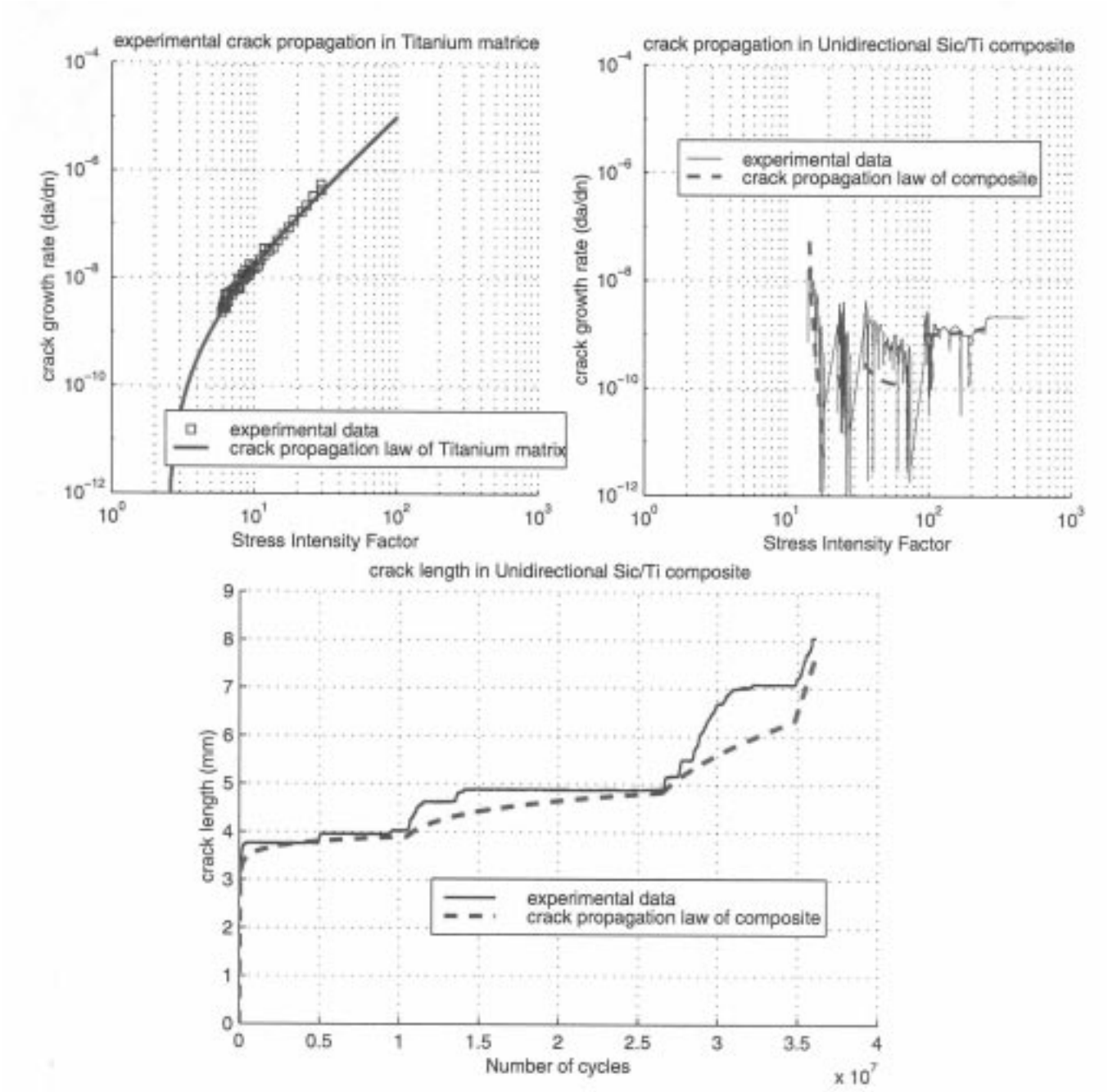

Figure 5: Comparison experimental data/model prediction for a room temperature test.

Determination of the crack growth rate

The equality between the expressions of the COD at the two scales (*Eqn.* 3 and *Eqn.* 5) provides the equation verified by the bridging pressure ***P(x)*** :

$$\Re_{micro}(P(x)) = {}^{1}\!/_{E^*} \int_{x}^{a} h(x,s,w).\left\{ \int_{0}^{s} h(t,s,w)\left(\sigma_a - P(x)\right)dt \right\} ds \qquad (6)$$

The resolution of *Eqn. 6,* at any stage of the loading allows to calculate ***P(x)*** along the matrix crack and to deduce ***ΔP(x)*** for a half cycle. Therefore ΔK_b and ΔK_{tip} can be calculated with *Eqn.* 2. Eventually, the crack growth rate is determined by the *Eqn.* 1.

As the number of cycles is high, we have preferred to use an incremental form on the crack length rather than on the number of cycles. For a given crack length ***a***, the equation 6 is solved twice to determine ***ΔP(x)***, a first time when $\sigma_a = \sigma_{\max}$, a second one when $\sigma_a = \sigma_{\min}$ and the crack growth rate is calculated with *Eqn.* 1. The procedure is repeated for each increment ***Δa***, which signifies that a mean crack growth is calculated over a range of ***dN*** cycles. This method appeared to be correct as long as there is no appreciable time

dependent effects over a period of ***dN*** on the constituent properties.

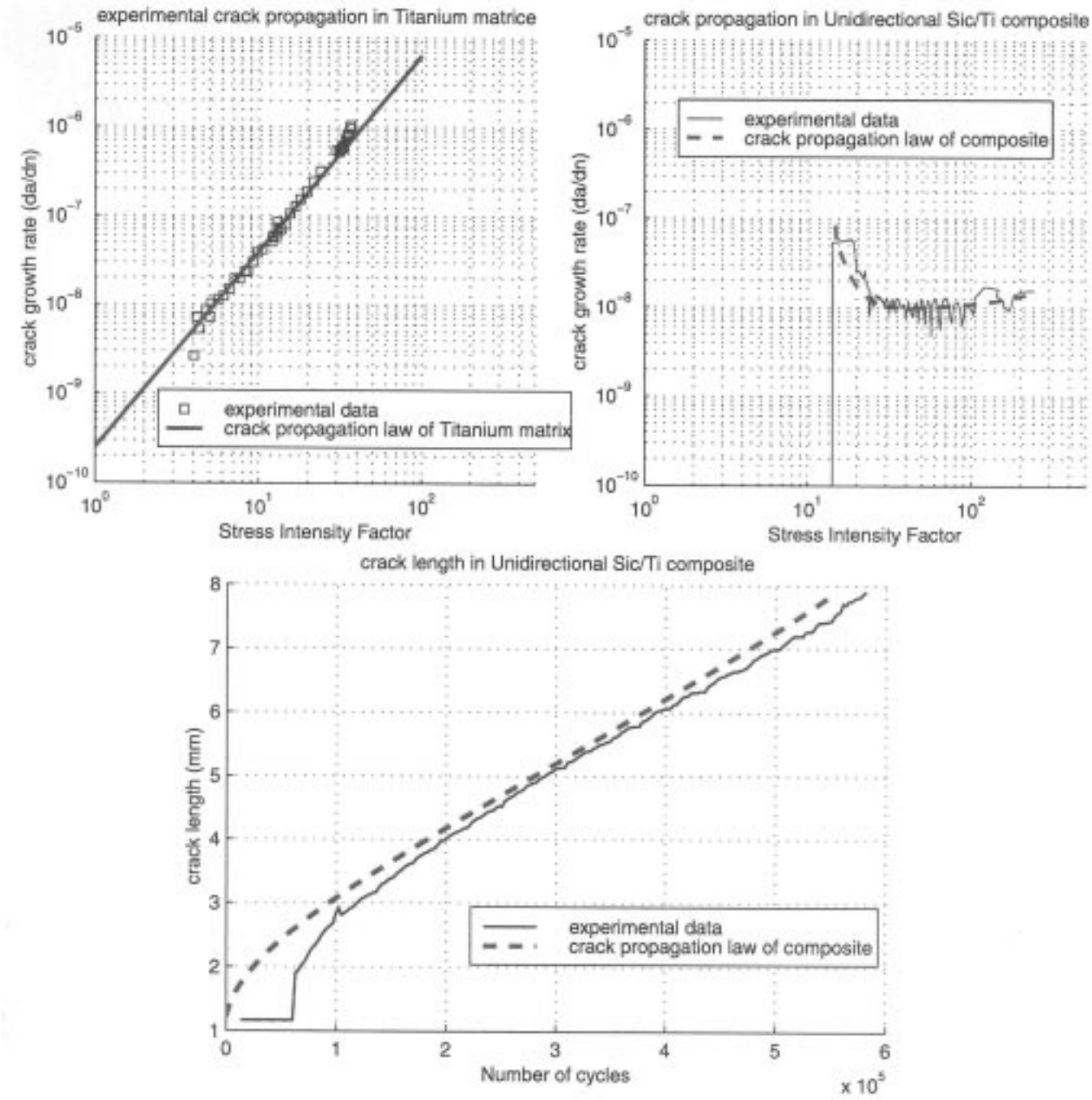

Figure 6: Comparison experimental data/model prediction for a high temperature test (400°C).

Model results

The fitting of the experiment gives an appropriate result. The trend of the crack growth is well described for each part: the initial deceleration, the steady state and the final acceleration. The behaviour of the elementary cell has been obtained from micromechanical tests (pull-out and push-out, Guichet [4]). Furthermore, the material parameters used to describe the propagation law for the titanium matrix are in agreement with the usual values (see table 1).

TABLE 1: coefficients of the propagation law for the Titanium Matrix

Room Temperature	Ks = 2.4	$c = 1\ 10^{-10}$	n = 2.5
High Temperature (400°C)	Ks = 0	$c = 2.5\ 10^{-10}$	n = 2.2

This model cannot describe the fluctuation at the cell size. However, at a macroscopic point of view, in order to predict the tolerance of the material, this issue appeared to be lesser important. This phenomenon is complex to model, the two scales interact each other and a more refine description is required. In that way, Xu et al have proposed a crack trapping model [17].
The abilities of this model are in agreement with the different experimental stages for room temperature tests (figure 5) and for high temperature tests (figure 6).

CONCLUSION

The bridging fibres exert significant effects on the fatigue crack propagation, reducing the growth rate in an appreciable way. Their performance depends on the behaviour of the fibre/matrix interface. The main characteristics of the proposed model is to take interfacial properties in to account, especially debonding and friction. This ability is of a great interest for the design of materials. The optimal properties of interface remain a complex problem and should be overcome by this kind of model.
On the other hand, direct expressions can be deduced from the results of this two-scale model. It requires analysing systematically the influence of the pertinent parameters. This could lead at term, to a macroscopic law for the bridged crack propagation.
Furthermore, experimental shapes with finite width and the presence of a notch can be treated. Other states than the usual state-steady have been described which allows further developments. For instance, the effects of fibre fracture could be analysed with a statistical approach, the fibre stress state being calculated by the model. The issue is necessary to evaluate the damage tolerance of these materials; such events can lead to a catastrophic failure. Other aspects for future developments are to incorporate matrix stress relaxation, effects for high temperature and hold time effects

Acknowledgements

Authors would like to thank Prof. H. Ghonem (Professor in Mechanics of Materials Laboratory, Department of Mechanical Engineering, University of Rhode Island) for its collaboration with our department and his valuable recommendations for the testing procedures. The support of SNECMA for the specimen manufacturing and the financial support of DGA (French Ministry of Defence) are also gratefully acknowledged.

References

1. Legrand N. (1997), Phd thesis, Ecole Nationale des Mines de Paris, France.
2. Naik R.A. and Johnson W.S. (1989), ***Composite Materials: Fatigue and Fracture***, pp. 753-771.
3. Ghonem H., Wen Y. and Zheng D. (1993), ***Applied Mechanics***, vol. 34, pp. 161-180, 1993.
4. Guichet B. (1998), Phd thesis, Ecole Centrale de Lyon, France.
5. Marshall D.B., Shaw M.C. and Morris W.L. (1992), ***Acta. Metal. Mater***., vol. 40, n° 3, pp. 443-454.
6. Fett T. (1996), ***Engineering Fracture Mechanics***, vol. 53, n° 3, pp. 363-370.
7. McMeeking R.M. and Evans A.G. (1990), ***Mechanics of Materials,*** vol. 9, pp. 217-227.
8. Ghonem H. (1998), in ***Titanium Matrix Composites,*** S. Mall and T. Nicholas, Eds.: Technomic.
9. Cotterill P.J. and Bowen P. (1993), ***Composites,*** vol. 24, n° 3, pp. 214-221.
10. Rice J.R. (1972), ***Int. J. Solids Structures,*** vol. 8, pp. 751-758.
11. Tvergaard V. (1990), ***Mat. Scienc. and Eng.,*** vol. A125, pp. 203-213.
12. Chaboche J.L., Girard R., and Schaff A. (1997), ***Computational Mechanics,*** vol. 20.
13. Chaboche J.L., Girard R., and Levasseur P. (1997), ***Int. J. Damage Mechanics,*** vol. 6.
14. Marshall D.B. and Oliver W.C. (1990), ***Mat. Scienc. and Eng.,*** vol. A126, pp. 95-103.
15. Hutchinson J.W. and Jensen H.M. (1990), ***Mechanics of Materials,*** vol. 9, pp. 139-163.
16. Marshall D.B., Cox B.N., and Evans A.G. (1985), ***Acta. Metall***., vol. 33.
17. Xu G., Bower A.F., and Ortiz M. (1998), ***J. Mech. Phys. Solids,*** vol. 46, n° 10, pp. 1815-1833.